Impact of wind on crash-landing mortality in grey-headed albatrosses *Thalassarche chrysostoma* breeding on Marion Island

Schoombie J[1], Schoombie S[2], Connan M[2], Jones CW[3], Risi M[3], Craig KJ[1], Smith L[1], Ryan PG[3], Shepard ELC[4]*

[1] *Department of Mechanical and Aeronautical Engineering, University of Pretoria, Pretoria 0028, South Africa*

[2] *Department of Zoology, Marine Apex Predator Research Unit (MAPRU), Institute for Coastal and Marine Research, Nelson Mandela University, Gqeberha 6001, South Africa*

[3] *FitzPatrick Institute of African Ornithology, University of Cape Town, Rondebosch 7701. South Africa*

[4] *Department of Biosciences, Swansea University, Swansea SA2 8PP, UK*

*Corresponding author: Janine Schoombie, janine.versteegh@gmail.com

Abstract:

Albatrosses exploit winds to travel vast distances across the ocean. Their morphology is adapted for low-cost dynamic soaring flight, but these adaptations confer low manoeuvrability, which may be risky when flying over land. This study investigates how wind conditions influence endangered grey-headed albatross *Thalassarche chrysostoma* crashes in the valley below an inland sub-colony on Marion Island. Carcass surveys were conducted in a 1 km^2 area spanning the length of this sub-colony (c. 4000 breeding pairs) from October 2017 to June 2021. Hundreds of adult and fledgling albatross carcasses were discovered, some with evidence of fatal crash-landings in the form of broken bones. Wind data measured on the cliff top above the colony were supplemented by computational fluid dynamics simulations of wind vectors over Marion Island. Most crashes occurred below the centre of the colony, where there are strong gradients in wind speed and direction under the dominant westerly wind conditions. Observations of albatrosses in flight indicate that most birds are killed when attempting to leave the colony, specifically when flying low above ground in strong wind. An average of at least 41 adults and 40 fledglings died after crashing into the valley annually. This represents an estimated 2% of the annual production of fledglings, 0.5% of the estimated annual breeding adult population and 11% of the adult annual mortality, suggesting a substantial cost to breeding at this inland site. For these long-lived seabirds, even low levels of adult mortality can have potential demographic consequences. This is the first study to document persistent wind-driven, land-based mortalities in albatrosses.

Keywords: flight limitations, seabird mortality, wind gradients, numerical modelling, demographic impact

1. INTRODUCTION

Seabirds are long-lived, with low levels of natural mortality. However, they are now one of the world's most endangered bird groups with over 30% of species globally threatened (BirdLife International 2022a). A global assessment recently concluded that interactions with fisheries, invasive species, extreme weather and climate change represent some of the main threats to seabirds (Dias et al. 2019). Procellariiformes are particularly well-studied, and the effects of bycatch in this group are relatively well documented (e.g., Robertson et al. 2014, Krüger et al. 2018, da Rocha et al. 2021). A range of species of albatrosses have also experienced predation by invasive mammals (Dilley et al. 2015, Work et al. 2021). Other land-based sources of mortality do occur, including predation by other seabirds (Risi et al. 2021) and landslides during extreme rain events (Ryan 1993).

Cone (1964) notes the possibility of albatrosses sustaining fatal injuries during high-impact, terrestrial landings. There are also anecdotal observations of crash-landings in day-flying species, some of which have been fatal, including in wandering albatrosses *Diomedea exulans* breeding at Marion Island and sooty albatrosses *Phoebetria fusca* on Gough and Inaccessible Islands (PG Ryan *pers. obs.*). Albatrosses are renowned for their ability to exploit winds in the Southern Ocean to fly vast distances with little flapping (Nel et al. 2001, Catry et al. 2004a, Weimerskirch et al. 2012, Tarroux et al. 2016, Richardson et al. 2018). Their adaptations to wind-soaring include high wing loading, which is associated with fast flight (Warham 1977, Suryan et al. 2008). These adaptations for flight over the ocean have the potential to become constraints when birds fly over land, as the combination of high body mass and fast flight means that momentary loss of flight could be fatal when these birds fly low over the ground.

Marion Island (290 km^2, 46.9° S, 37.75° E), the larger of the two Prince Edward Islands, is home to c. 8% of the world population of grey-headed albatrosses *Thalassarche chrysostoma* (Ryan et al. 2009, BirdLife International 2022b). These albatrosses breed in several sub-colonies on the island, including along an east-facing inland cliff where c. 4000 pairs breed in nests that are sheltered from the predominant westerly winds. One study plot in this sub-colony (69-131 breeding pairs; FitzPatrick Institute of African Ornithology [FIAO] unpubl. data) has been monitored since 1996 to document breeding success (Ryan et al. 2007) and survival (Converse et al. 2009). In 2017, grey-headed albatrosses were observed crashing into the valley below this inland sub-colony. A subsequent survey found hundreds of carcasses of grey-headed albatrosses (adults and fledglings) in an area of c. 1 km^2, many of which had signs of impact, such as broken wings, legs, necks, and bills, suggesting these birds crash-landed. In this study we (1) document the number of grey-headed albatross crashes and assess the demographic implications by comparing this to estimated adult mortality and (2) assess the particular wind conditions that might be responsible for crashes, using crash locations, a computational fluid dynamics model of wind over Marion Island, and observations of albatross flight behaviour under varying wind conditions. Overall, this should provide new insight into the wind conditions that may cause loss of flight control in these wind-adapted seabirds, as well as the implications of this cause of mortality in an important breeding site.

2. METHODS

2.1. Crash mortality

Grey-headed albatrosses breed in dense colonies on steep slopes on sub-Antarctic islands (Pennycuick 1982, Waugh et al. 1999, Catry et al. 2004b). Approximately

4500 breeding pairs breed on the southern coastal cliffs of Marion Island and another c. 4000 pairs breed on an inland cliff, aptly called Grey-headed Albatross Ridge (hereafter referred to as the Ridge; Risi et al. 2019, FIAO unpubl. data). The Ridge extends c. 2 km inland from the south coast of Marion Island and supports multiple sub-plots of different sizes and altitudes, with the highest sub-plot c. 240 m above sea level (Dilley et al. 2015). To the West of the Ridge is an extended plateau that slopes slightly down toward the Ridge (Fig.1). The valley to the east of the Ridge, Santa Rosa Valley (hereafter referred to as the Valley), is characterised by rugged black lava with little vegetation (Rudolph et al. 2022).

A 1 km^2 section of the Valley was surveyed for grey-headed albatross carcasses for four breeding seasons from October 2017 to June 2021. The western edge of the survey area ran along a drainage line at the base of the cliff (Rudolph et al. 2022), from the southern tip of the Ridge to the northern-most grey-headed albatross nests and extended c. 200 m east (Fig. 1). This eastern limit was estimated by preliminary observations of stranded birds and the flight paths of the birds along the Ridge. To be conservative, any carcasses to the west of the drainage line (i.e., immediately below the cliff) were excluded as these mortalities may have occurred on the Ridge (e.g. due to predation or disease). The following was recorded for each carcass: GPS location, age class (‘adult’, ‘fledgling’ or ‘unknown’ if it could not be aged reliably), carcass condition (level of decay) and evidence of injuries (e.g. broken bones), where the age and state of the carcass allowed. A detailed description of the carcass condition and age classification is given in the supplementary material (Appendix A and Fig. S1).

In October 2017, an exhaustive search was conducted to remove all old carcasses from the study area. In subsequent surveys, the location of each new carcass was

recorded using a hand-held GPS. Carcasses were buried under rocks and the data were inspected for possible duplicates after each survey. During surveys, live albatrosses present in the study area were also recorded with information on any injuries.

Five to 6 carcass surveys were completed during each breeding season (except for 2019/20, where 9 surveys were completed from late August 2019 to April 2020), with counts spread approximately evenly across the season. The period between each count varied from 20 – 30 days. Fresh carcasses or live albatrosses observable from the Ridge or the field hut were also recorded in-between surveys when other work was conducted in the area. Due to the COVID-19 pandemic restrictions, access to the site was not possible in May and June 2020. The next survey was carried out in late October 2020.

The locations of all carcasses, including the initial clearance, were used for spatial analysis of crashes, but only new crash events (i.e. crash events occurring within the study period) were used in the assessment of mortality rates. To be conservative, all old carcasses were considered crash events that occurred before the study period. Not all crashes resulted in instantaneous death or severe injuries. Some birds were observed attempting to take off again from the Valley, but we could not confirm how many were able to do this successfully and how many died of other causes or crashed in a different location.

Density maps were created of all (old and new) recorded grey-headed albatross crash locations. In most cases, it was unknown whether live albatrosses crashed where they were found, so their locations were excluded from the spatial analysis. A kernel density estimation was applied to the dataset and interpolated onto an evenly

spaced 10 x 10 m grid using the R-package *ks* (Duong 2007). A symmetric Gaussian kernel was used, and the bandwidth was calculated using the method of Wand & Jones (1993) and Duong & Hazelton (2003).

Albatrosses were most numerous at colonies at the start of the breeding season, when established breeders returned to breed, and pre-breeders looked for mates and nest sites. The latter birds were particularly active, often taking off and landing at different colonies (Tickell 1984, J Schoombie pers. obs.). Most grey-headed albatrosses arrived at Marion Island in late August or early September, similar to South Georgia (Clay et al. 2016), with experienced breeders typically arriving first (Tickell 1984), and non- and pre-breeders arriving slightly later (Tickell & Pinder 1975, Stahl & Sagar 2006). Egg laying mostly occured in the first week of October and incubation lasted until late December (Ryan et al. 2007, Ryan & Bester 2008). On Marion Island, foraging trips lasted 8–28 days during incubation (Nel et al. 2000, Carpenter-Kling et al. 2020) and c. 4 days during brood-guard and early chick-rearing (Nel et al. 2000). The brood-guard phase ended in late January and all surviving chicks were left unattended by the first week of February. Chick provisioning continued until mid-May when the first chicks fledged. On Bird Island, South Georgia, grey-headed albatross trip durations increased towards fledging (Huin et al. 2000). Adults typically spent 5–10 minutes at the nest after relieving their partner or feeding the chick (Tickell 1984). Few adults visited the island after the end of May, and most fledglings had departed by mid-June.

Annual counts of incubating breeding pairs (late October to early November, Ryan et al. 2009) and fledglings (late April) were available from the entire sub-colony (i.e., the Ridge) for all four breeding seasons (2017/18 to 2020/21). Nest occupancy counts, which include nests occupied (NO) by non-breeders (Ryan et al. 2007, 2009), were

used as a minimum estimate of adult grey-headed albatrosses present (AP) (where AP = NO x 2). Crash fatalities were compared to the number of adults and fledglings counted during each breeding season. An estimate of annual adult mortality (AAM) was calculated using a survival rate of 95.1% (Converse et al., 2009) and the estimate of adults present (AAM = [1 – 0.951] x AP). The number of adult crash fatalities in the Valley is reported as a proportion of the estimated annual adult mortality. The number of fledgling crash fatalities is reported as a proportion of the annual chick production.

2.2. Wind data

Several features of the wind field around the Ridge could present potential problems for albatrosses in flight. For instance, variable wind vectors could lead to a loss of lift, downdrafts could cause a loss of altitude and turbulence could adversely affect their control/stability. Alternatively, crashes could have simply been linked to particular wind vectors. Several approaches were used to investigate the wind characteristics associated with crash events.

A network of wind sensors was installed at 17 locations on Marion Island in 2018 (Goddard et al. 2022), including one at the top of the Ridge (Fig. 1). A two-dimensional sonic anemometer (*GILL WindSonic* ^{TM}) was mounted on a mast 1 m above ground level (m.a.g.l.) in the centre of the breeding cliff (46.9560° S, 37.70595° E, c. 210 m.a.s.l.). Wind speed and direction were measured at 0.5 Hz and data were stored as 10 min, hourly and daily averages. Hourly wind averages were used for analyses unless stated otherwise.

In the absence of accurate gust measurements at the Ridge, the 98th percentile was used to determine the upper threshold for extremely strong winds (Pinto et al. 2007,

Louzao et al. 2019). For comparison, the 2nd percentile wind speed was used as the threshold for calm conditions. The number of extreme wind events was then compared to the number of new crash events for a given period.

Three-dimensional data from computational fluid dynamics (CFD) simulations, sourced from Goddard et al. (2022), were used to create fine-scale wind maps around the Ridge and the Valley. The CFD simulations solved the steady Reynolds-averaged Navier-Stokes (RANS) equations to provide pressure and velocity fields of air flowing over a three-dimensional high resolution digital model of both Marion and Prince Edward Island (Goddard et al., 2022). The nature of the CFD simulations was such that a specific wind condition was imposed on a volume of air surrounding Marion Island (freestream condition), which included the logarithmic velocity gradient that models the atmospheric boundary layer. While turbulent eddies were not fully resolved in these steady RANS simulations, the isotropic turbulence intensity (TI) was estimated mathematically using turbulence closure schemes, which provided insight into areas of higher and lower turbulence as may be experienced by birds. As described in Goddard et al. (2022) the wind speed measurements from Marion Island were used to estimate the inlet TI profile for the CFD simulations at the inlet boundary condition. The CFD data extracted directly from the simulations were interpolated to an equally spaced 60 x 60 m grid to visualise wind patterns within the study area for a sample of eight cardinal wind directions. Measurements at the top of the Ridge were representative of the freestream CFD condition (Goddard et al. 2022). Therefore, a simulated westerly wind will give details of the fine-scale wind velocity and TI surrounding the Ridge when the wind sensor on top of the Ridge also recorded a westerly wind (see Goddard et al., 2022 supplementary material).

Throughout this paper, we will use the phrase “variable wind” to mean large spatial changes in velocity vectors that describe the time-averaged flow. Where “turbulence” is used it refers to the TI as calculated by the RANS CFD model.

2.3. Flight behaviour

Observations were made to document grey-headed albatross crashes in the Valley and link them to wind conditions and flight behaviour. Two methods were employed: (1) direct observations of grey-headed albatrosses in flight, where focal individuals were followed in a range of wind directions and (2) camera observations, involving the installation of two time-lapse cameras that recorded strategic areas of the Valley from the top of the Ridge (Fig. 1).

During direct observations, the trajectories of birds flying near the breeding ridge were documented, along with estimates of flight height. The grey-headed albatross breeding colonies are typically located on gentle, terraced slopes on the upper and middle sections of the Ridge. Below these sloped colonies is a sheer cliff down to the Valley. The top of the Ridge and the top line of the cliff face was used to estimate the height of flying albatrosses relative to the ground. Direct observations were carried out from observation points on the Ridge outside the colony to avoid disturbing nesting birds (Fig. 1). Observations were carried out for 1-2 hours during pre-laying and incubation from August – December 2019.

Any crash landings during the direct observations were recorded and linked to the wind conditions on the Ridge, taken as the average of the 10-minute wind speed and direction values before and after the time of impact. At the start of each observation period, the Valley was scanned from the viewpoint on top of the Ridge for live albatrosses. If a live albatross was subsequently observed in the Valley (during or at

the end of the observation period), where it was known that the bird had crash-landed within the past two hours, the average wind speed and direction were reported for the preceding two hours.

Three cameras (*Wingscapes® TimelapseCam Pro*) were installed on the Ridge well outside grey-headed albatross nest sites to avoid disturbance of breeding birds (Fig. 1). Videos of sections of Santa Rosa Valley were recorded for 10 seconds at 15-minute intervals from 8:00 to 17:00 every day in March 2020 – May 2021. Videos were inspected for crash events (crash landings or live birds). The 10-minute averaged wind data for the date and time of each crash event were obtained from the anemometer on top of the Ridge and a mean is reported for the preceding two hours.

All data analyses were performed in the R statistical environment (R version 4.1.0; R Core Team, 2021).

3. RESULTS

We found 91 carcasses during the initial clearance survey in October 2017: 34 adults (14 new and 20 old), 20 fledglings (all old) and 37 old carcasses that could not be aged. Subsequent surveys found 470 carcasses. However, 87 of these were old carcasses that were probably missed during the initial clearance survey, giving a minimum of 383 new mortalities from October 2017 to June 2021: 184 adults, 174 fledglings and 25 that could not be aged (due to missing heads). Together with the 14 new crash events collected in October 2017, this gives an average of 41 adult and 40 fledgling mortalities per year (Table 1). The cause of death for birds crash-landing in the Valley could not be verified in all cases but evidence of injuries such

as broken bones and bleeding were recorded for 29 live birds/fresh carcasses. Many more could have incurred injuries, but the proportion cannot be reported reliably due to the state of decay in the carcasses. One live adult observed in the Valley had no obvious injuries (but had regurgitated material next to it). Carcasses of 6 sooty albatrosses and 2 giant petrels *Macronectes* spp*.* were also observed in the study area but were excluded from this study.

The mean number of occupied nests on the Ridge was 3860 ± 171 per year. Adult crash fatalities therefore represented c. 0.5% of adults at the Ridge (Table 1). Annual chick production averaged 1785 ± 244, so fledgling crash mortality represented c. 2% of fledglings (Table 1). During the 2019/20 breeding season, when sampling was most frequent, crash events mainly occurred at the start of the breeding season (Fig. 2). From November to March, there was a consistent number of new crash events observed in the study area, decreasing to only 2 in April 2020 when the last survey was completed for the 2019/20 breeding season.

3.1. Predictors of crash events

The dominant wind direction at the top of the Ridge was from the western quarter (south-west to north-west, Fig. 2a). However, the strongest winds (mean hourly speeds ≥ 14 $m.s^{-1}$ and hourly maxima ≥ 24 $m.s^{-1}$, Fig. 2a) tended to be associated with northerly winds, while southerly winds were often lower (mean hourly speeds ≤ 6 $m.s^{-1}$). The 98^{th} and 2^{nd} percentile of the average hourly wind speeds were 12 $m.s^{-1}$ and 1 $m.s^{-1}$, respectively. There was no clear relationship between the number of carcasses and the frequency of calm or strong wind speed measurements (Fig. 2c).

There were insufficient data on visitation rates by adults or the changing numbers of breeding and non-breeding adults through the season to accurately model the effect

of the number of colony visits on observed crash rates. However, the decrease in crashes through chick-rearing does correspond to the observed decrease in the number of adults visiting the colony per day during this period (see also Huin et al. 2000).

Sixteen crash events (10 adults and 6 fledglings) were observed directly between August 2019 and January 2020 or via the *Wingscapes*® camera footage from March 2020 to February 2021. In the observed adult crash events the wind direction was predominantly from the west (214° - 322°, Fig. 2b) (wind speeds 3.8 - 10.9 $m.s^{-1}$). In 3 cases, a portion of the adult albatross's flight path was observed before it crashed. In these 3 cases, the birds flew south (departing toward the ocean) and flew low over the Valley. The 6 fledgling crashes occurred across a wide range of wind directions (118° - 327°) and speeds (1.2 – 8.3 $m.s^{-1}$).

Fledglings and adults both tended to crash in the same area (supplementary material, Fig. S2) and there was a clear hotspot of crash sites near the centre of the study area (Fig. 3a), c. 80 m east of the base of the Ridge. Under the prevailing westerly winds, this hotspot coincided with a region of highly variable flow in the lee of the Ridge (Fig. 3b) up to 20 m.a.g.l. (Fig. S11), with wind gradients rotating from 90° to 270° within <100 m. This variability was associated with downdrafts up to c. 50% of the velocity magnitude (Fig. 4a), even though wind speeds were very low in general at this height (speed << 1 $m.s^{-1}$), as is expected of the highly rotational flow in the lee of a bluff body (Fig. 4a and Fig. S3). This low-speed variable flow had mostly dissipated by 100 m.a.g.l. (Fig. 4a).

A similar volume of highly variable wind was present in south-westerly (Fig. S10) and north-westerly winds (Fig S12). As with a westerly wind, wind from the south-west

caused recirculating flow immediately to the east of the Ridge (Fig. S10 and Fig. 4a), generating both updrafts and downdrafts across the study area up to c. 20 m.a.g.l. (Figs. S10 & S11). Pockets of high turbulence were distributed through the survey area for both westerly and south-westerly winds. While relatively low at 1 m.a.g.l., the turbulence was still highest in the area surrounding the crash hotspot (Fig. S4a).

Wind flowing from the north-west seemed to be diverted around the interior and arrived in the Valley from the north-east, colliding just north of the crash hotspot, resulting in an area of very low speed and a sharp gradient in turbulence across the carcass hotspot (Fig. S12).

The simulated wind vectors were less variable over the study area in north-easterly (Fig. 3c and Fig. S6) and south-easterly winds (Fig. S8. Winds with a strong easterly component (Fig. S7) caused updrafts as air flowed over the Ridge (Fig. 4b). Despite high turbulence levels across the study area with easterly winds (and increasing with altitude), the turbulence remained relatively consistent spatially (Fig. S7c). Wind directly from the north resulted in small pockets of high variability in speed with a fairly constant direction (Fig. S5). This high variability of wind speed and TI could be attributed to the presence of the high peaks (c. 1000-1300 m.a.s.l.) c. 6 km north of the crash hotspot (Fig. 1).

3.2. Effect of wind on flight paths

In general, adult grey-headed albatrosses arrived at the colony from a relatively high altitude and looped down to land into the wind. The approach to landing usually followed a figure-of-eight pattern but could also be a circular loop (Fig. 5). Departing birds usually walked to exposed positions to take off into the wind, swiftly turning south toward the ocean (Fig. 5e).

The number of albatrosses observed flying along the Ridge tended to be greatest (many hundreds) during light winds (≤ 3.5 $m.s^{-1}$) from an easterly and south-easterly direction. Under these conditions, birds took off into a headwind from the east-facing cliffs (Figs. 5e, S7 and S8), and quickly gained altitude, often without flapping. In contrast, landings were more challenging with an easterly wind as they needed to approach from the west and attempt to land on a downward slope to avoid landing with a tailwind (Fig. 5b). Albatrosses flew in loops over the Ridge to land facing east, although they did not lose much altitude when aborting a landing attempt due to the available headwind and updrafts (Fig. 4b).

In northerly winds, the Valley is in the lee of the high interior peaks of the island (Fig. 1), which caused variability in wind speed and direction in the study area and relatively high turbulence to the west of the crash hotspot (Fig. S5c). In light to moderate northerly winds, albatrosses arrived above the top line of the Ridge and looped multiple times over colonies to land facing north (Fig. 5a). However, northerly winds were often characterised by high wind speeds (> 6.5 $m.s^{-1}$, Fig. 2a). The few observations of albatrosses flying in these conditions (< 10 individuals) were all of birds departing the colony, flying south along the Ridge toward the ocean (Fig. 5e) below the colony slopes. The strong tailwind resulted in very high ground speeds and several birds appeared to have little control (erratic wing movements and rolling), which may have been caused by high turbulence (Fig. S5c). Albatrosses attempting to access their nests in the strong headwind were forced to walk north at the top of the Ridge (https://vimeo.com/716680131).

Many birds (tens to hundreds) were observed flying along the Ridge during westerly winds, noticeably less than during easterly winds. When arriving from the ocean, albatrosses were often observed to turn east when above the Ridge and dive,

gaining speed to turn very rapidly at low altitude toward the west, rising toward the colony and land facing west (Fig. 5d). However, take-offs toward the east exposed the birds to a tailwind, and probably a downdraft (see Fig. 4a), reducing airspeed and albatrosses were observed to wait for long periods for ideal take-off conditions (i.e., headwinds or updrafts). The albatrosses flapped hard when taking off and lost a great deal of altitude before turning south and heading to the ocean (Fig. 5e).
In south-westerly winds, the study area was in the lee of the tip of the Ridge and most horizontal variation in wind speed and direction was caused by the flow of air around this tip (Fig. S10). With southerly winds, the study area was not in the lee of any significant geographical structure (Fig. S9) though some wind speed and direction variability did exist to a lesser extent. Albatrosses could take off facing south, aided by a headwind and possibly light updrafts (Fig S9b) to remain airborne post-takeoff (Fig. 5e). Albatrosses returning from the ocean flew in loops around their colonies to land facing south (Fig. 5c). Large numbers (tens to hundreds) of birds were observed flying along the ridge during southerly winds, similar to westerly winds.

4. Discussion

In this study, we identified wind phenomena associated with fatal crash landings in grey-headed albatrosses on land. Over four breeding seasons (2017 to 2021), at least 198 adult grey-headed albatrosses crashed in a 1 km^2 study area below a sub-colony of c. 4000 breeding pairs on Marion Island, resulting in at least 163 fatalities. This is a minimum estimate of crash fatalities because some crashes may have occurred outside the search area, and other carcasses may have been overlooked. Collision mortality for seabirds has largely been recorded for offshore collisions with

vessels, oil platforms and wind farms (Johnston et al. 2014, Ronconi et al. 2015, Coleman et al. 2022). Both adult and fledgling seabirds are affected by artificial light, which can lead to fatal collisions with man-made structures (Black 2005, Rodríguez et al. 2017, Guilford et al. 2018). Studies on smaller seabirds have also shown that wind can adversely affect the birds' ability to land on cliff nests (Mallory et al. 2009, Shepard et al. 2019). Our results reveal a novel form of collision risk.

Given an adult survival rate of 95.1% (Converse et al. 2009), the adult crash-related mortalities represented c. 4-16% of annual natural mortality for grey-headed albatrosses breeding on the Ridge (Table 1). Although we note that the other c. 50% of Marion Island's population of grey-headed albatrosses breed on coastal cliffs and would therefore be much less vulnerable to crashing (some may crash into the sea on departure, but this is less likely to result in significant injuries).

The regular carcass surveys in the 2019/20 breeding season did not show a clear influence of extreme wind speeds or calm conditions on the number of new carcasses recorded (Fig. 2). Indeed, the number of crashes decreased throughout the chick-rearing period, despite an increase in the number of extremely high and low winds towards the end of this period. However, more adults fly along the Ridge early in the breeding season (Tickell 1984, pers. obs.), when more crashes were recorded, and adult visitation decreases toward the end of chick-rearing (Huin et al. 2000, Tickell 2000). It is therefore difficult to assess the role of extreme winds against the backdrop of seasonal changes in visitation rates.

Nonetheless, the fact that the crash hotspot coincided with an area of highly variable wind vectors and downdrafts, suggests that wind conditions were likely causing albatross crashes. Birds appeared most at risk when they departed the colony for the

sea, as departing albatrosses tended to lose altitude immediately after take-off, in contrast to returning birds, which typically arrived at higher altitudes. In support of this, all observed adult mortalities appeared to have been birds leaving the colony. Furthermore, adults crashed in the same area as fledglings (Fig. S2), and fledglings only departed to the sea without appearing to return to the colony (Frankish et al. 2022). The increased risk on departure may reflect challenging conditions along their particular trajectories, but they might also be influenced by the conditions under which adults elect to arrive at the colony. Adults returning to relieve partners from incubation or brooding duties, or to feed larger chicks, have the option to wait offshore until conditions for landing at the colony fall within acceptable limits. However, once relieved or having fed their chick, adults may have a greater incentive to depart the colony. If the conditions that favour arrival are less than ideal for departure, this inequality could exacerbate the risk of crashing on departure.

During departures, we propose that temporal and spatial variability in wind speed and direction (and possibly turbulence) puts low-flying albatrosses at risk of crash-landing. Variability in speed and direction was present in the Valley in all wind directions, but the degree of this variation appeared to be greater in westerly winds. In the predominant westerly winds, albatrosses flying low (≤ 20 m.a.g.l.) over the Valley near the Ridge may experience sudden changes in wind speed and direction and turbulence across their flight path. This variability, together with the presence of downdrafts (Fig. 4a), may cause birds flying low over the Valley to experience sudden loss of lift, thus losing altitude and leading to crash-landings. While it is difficult to distinguish between the variability of the horizontal component and downdrafts as the drivers for crashes, the magnitude of the horizontal variability was much greater than the strength of the downdrafts (Fig. 4). In reality both may be

problematic, particularly considering that both will vary in space and time as variable wind vectors approach the island.

In winds with a strong westerly component, albatrosses may also experience risky flight conditions on their approach to landing as they were observed looping low over the Valley at high speeds to turn west for a headwind landing on the Ridge (Fig. 5d). It is possible that they are also vulnerable to crash-landings during these turns, as sudden changes in wind direction and speed at low altitudes might result in a loss of airspeed (and thus lift), as reported for sailplanes in similar scenarios (Anderson 2008, US Department of Transportation 2013). Like sailplanes, grey-headed albatrosses also use wind shear and updrafts to soar over land instead of frequent flapping (Pennycuick 1982, Sachs et al. 2013, Richardson 2015, Bonnin et al. 2016, J Schoombie pers. obs.). So, if we were to treat a grey-headed albatross in flight as a sailplane, its morphology would also have a limited range of airspeeds and associated altitudes from which it can safely recover (Anderson 2008).

Breeding albatrosses are central-place foragers that are constrained to return to their nests to incubate eggs or feed chicks (Tickell 2000). The frequency of foraging trips depends on the breeding stage, with the longest trips during incubation and the shortest trips during the brood-guard period shortly after hatching (Tickell 2000, Nel et al. 2000). In the open ocean, seabirds are able to adjust their routes and flight speed in relation to wind fields (Shepard et al. 2016, Cornioley et al. 2016) and may also be able to choose more beneficial wind conditions when commuting to and from nests on land (Kranstauber et al. 2015, Taylor et al. 2016, Ventura et al. 2020). Adult albatrosses might be pressured to depart the colony in unfavourable conditions by the needs of their chick. This could happen more often during the brood-guard period when small chicks have to be fed more frequently (c. daily) and the adults

sometimes neglect their own body condition in favour of their offspring (Catry et al. 2006).

More than 75% of grey-headed albatross breeding pairs on the Ridge are located north of the location with the highest crash site density (Fig. 3). Only two small nesting areas (N ≤ 200 pairs) lie south of the 0.5 density contour line. Thus, the majority of the breeding albatrosses arriving or departing over the Valley (east of the Ridge) pass over the crash hotspot. This raises the question of why albatrosses breed on an inland ridge associated with a relatively high risk of fatal crashes? Despite its inland location, the Ridge provides opportunities for efficient commuting flight, take-offs and landings in terms of wind conditions. The prevailing westerly winds provide favourable conditions for landing on east-facing slopes, and the Ridge provides shelter for chicks from the dominant winds. However, the highly variable flow in the lee of the ridge cliffs causes disturbances to birds in flight and contributes to the mortality of adult grey-headed albatrosses. There may be a trade-off between risk in commuting flight and sheltering chicks from severe weather. On neighbouring Prince Edward Island, grey-headed albatrosses only breed on the northern coast, with most breeding on steep, north-east-facing slopes that extend from the coast to c. 500 m inland (Ryan et al. 2003). Wind measurements and computational wind simulations on Prince Edward Island could confirm whether these cliffs provide shelter from prevailing conditions and whether a similar trade-off exists on these inland cliffs.

Fledglings on the Ridge may benefit from shelter while on the nest, but they may also experience difficult flight conditions on their first departure to the sea, depending on the wind conditions at the time of take-off. The 40 fledgling crash mortalities per year represented 2% of the chick production on the Ridge. This is clearly higher than

0.5% of adults that crash, suggesting that fledglings experience greater risks, particularly given that these crashes must have occurred during their first flight (Frankish et al. 2022). Poor body condition or lack of flying experience could well contribute to the likelihood of fledglings landing in the Valley (Corbeau et al. 2020, Collet et al. 2020). Unfortunately, we could not verify the health of any of the chicks that crashed before fledging but given that fledglings would have been aiming to reach the ocean, any intrinsic effects are likely to have been exacerbated by adverse wind conditions.

In summary, we showed that land-based mortality, in the form of fatal crash landings, contributed 11% of the natural mortality of adult grey-headed albatrosses at an inland sub-colony on Marion Island, and decreased chick production by around 2% (which is less significant demographically than adult mortality, given the generally low chick production per pair, as observed on Campbell Island; Waugh et al. 1999). Crash landings were most likely caused by highly variable wind conditions in a specific area, mostly impacting birds departing the breeding colony when they flew low to the ground in the dominant, westerly wind direction, as well as north-westerlies. Increased occurrences of strong northerly winds on Marion Island (le Roux 2008) have been attributed to the poleward shift in the Southern Ocean Westerlies (Weimerskirch et al. 2012). If this trend continues, the likelihood that grey-headed albatrosses breeding on the Ridge will be forced to depart nests in unfavourable conditions may also increase. While continued surveys are required to monitor the effect of changes in wind conditions over the long term, the current level of wind-related mortality in grey-headed albatrosses is substantial for a long-lived species with a low natural mortality rate.

Acknowledgements

Special thanks to Prof. Peter le Roux (University of Pretoria, Dept. Plant and Soil Sciences) for logistical support and wind data. We also thank all field workers who collected data over the study period: Dineo Mogashoa, Elsa van Ginkel, Monica Leitner, Charlotte Heijnis, Sean Morar, Oyena Masiko, Michelle Thompson, Jenna van Berkel, Leandri de Kock, Danielle Keys, Eleanor Weideman, Isabel Micklem, Yinhla Shihlomule and Lucy Smyth. Financial and logistical support was provided by the South African National Antarctic Programme (grant no. 110726, 110738 and 129226) and the Department of Forestry, Fisheries and the Environment.

Literature cited

Anderson JD (2008) Introduction to flight, 6th ed. McGraw-Hill, New York.

BirdLife International (2022a) State of the World's Birds 2022: Insights and solutions for the biodiversity crisis. Cambridge, UK: BirdLife International

BirdLife International (2022b) Species factsheet: *Thalassarche chrysostoma*. Downloaded from http://www.birdlife.org on 28/09/2022.

Black, A. (2005). Light induced seabird mortality on vessels operating in the Southern Ocean: Incidents and mitigation measures. Ant Sci 17: 67-68.

Bonnin V, Benard E, Toomer CA, Moschetta J-M (2016) Dynamic soaring mechanisms in the ocean boundary layer. International Int J Eng Syst Model Simul 8:136–148.

Carpenter-Kling T, Reisinger RR, Orgeret F, Connan M, Stevens KL, Ryan PG, Makhado A, Pistorius PA (2020) Foraging in a dynamic environment: Response

of four sympatric sub-Antarctic albatross species to interannual environmental variability. Ecol Evol 10:11277–11295.

Catry P, Phillips RA, Croxall JP (2004a) Sustained fast travel by a Gray-headed Albatross (*Thalassarche chrysostoma*) riding an Antarctic storm. Auk 121:1208–1213.

Catry P, Phillips RA, Phalan B, Silk JRD, Croxall JP (2004b) Foraging strategies of grey-headed albatrosses *Thalassarche chrysostoma*: integration of movements, activity and feeding events. Mar Ecol Prog Ser 280:261–273.

Catry P, Phillips RA, Forcada J, Croxall JP (2006). Factors affecting the solution of a parental dilemma in albatrosses: at what age should chicks be left unattended? Anim Behav 72:383–391.

Clay TA, Manica A, Ryan PG, Silk JRD, Croxall JP, Ireland L, Phillips RA (2016). Proximate drivers of spatial segregation in non-breeding albatrosses. Sci Rep 6:29932.

Coleman J, Hollyman PR, Black A, Collins MA (2022) Blinded by the light: Seabird collision events in South Georgia. Polar Biol 45:1151–1156.

Collet J, Prudor A, Corbeau A, Mendez L, Weimerskirch H (2020) First explorations: ontogeny of central place foraging directions in two tropical seabirds. Behav Ecol 31:815–825.

Cone, CD (1964) A Mathematical Analysis of the Dynamic Soaring Flight of the Albatross with Ecological Interpretations. Special scientific report 50. Virginia Institute of Marine Science, College of William and Mary.

Converse SJ, Kendall WL, Doherty PF, Ryan PG (2009) Multistate models for estimation of survival and reproduction in the grey-headed albatross (*Thalassarche chrysostoma*). Auk 126:77–88.

Corbeau A, Prudor A, Kato A, Weimerskirch H (2020) Development of flight and foraging behaviour in a juvenile seabird with extreme soaring capacities. J Anim Ecol 89:20–28.

Cornioley T, Borger L, Ozgul A, Weimerskirch H (2016) Impact of changing wind conditions on foraging and incubation success in male and female wandering albatrosses. J Anim Ecol 85:1318–1327.

Dias MP, Martin R, Pearmain EJ, Burfield IJ, Small C, Phillips RA, Yates O, Lascelles B, Borboroglu PG, Croxall JP (2019) Threats to seabirds: A global assessment. Biol Conserv 237:525–537.

Dilley BJ, Schoombie S, Schoombie J, Ryan PG (2015) 'Scalping' of albatross fledglings by introduced mice spreads rapidly at Marion Island. Antarct Sci 28:1–8.

Duong, T (2007) ks: Kernel Density Estimation and Kernel Discriminant Analysis for Multivariate Data in R. J Stat Softw 21: 1–16.

Duong T, Hazelton M (2003) Plug-in bandwidth matrices for bivariate kernel density estimation. J Nonparametr Stat 15:17–30.

Frankish CK, Manica A, Clay TA, Wood AG, Phillips RA (2022) Ontogeny of movement patterns and habitat selection in juvenile albatrosses. Oikos 2022:e09057

Goddard KA, Craig KJ, Schoombie J, le Roux PC (2022) Investigation of ecologically relevant wind patterns on Marion Island using Computational Fluid Dynamics and measured data. Ecol Modell 464:109827.

Guilford T, Padget O, Syposz M (2018) Light pollution causes object collisions during local nocturnal manoeuvring flight by adult Manx Shearwaters Puffinus puffinus. Seabird 31:48–55

Huin N, Prince PA, Briggs DR (2000) Chick provisioning rates and growth in Black-browed Albatross *Diomedea melanophris* and Grey-headed Albatross *D. chrysostoma* at Bird Island, South Georgia. Ibis 142:550–565.

Johnston A., Cook ASCP, Wright LJ, Humphreys EM, Burton NHK (2014) Modelling flight heights of marine birds to more accurately assess collision risk with offshore wind turbines. J Appl Ecol, 51: 31-41.

Kranstauber B, Weinzierl R, Wikelski M, Safi K (2015) Global aerial flyways allow efficient travelling. Ecol Lett 18:1338–1345.

Krüger L, Ramos JA, Xavier JC, Grémillet D, González-Solís J, Petry M v., Phillips RA, Wanless RM, Paiva VH (2018) Projected distributions of Southern Ocean albatrosses, petrels and fisheries as a consequence of climatic change. Ecography 41:195–208.

Louzao M, Gallagher R, García-Barón I, Chust G, Intxausti I, Albisu J, Brereton T, Fontán A (2019) Threshold responses in bird mortality driven by extreme wind events. Ecol Indic 99:183–192.

Mallory ML, Gaston AJ, Gilchrist HG (2009) Sources of Breeding Season Mortality in Canadian Arctic Seabirds. Arctic 62:333–341.

Nel DC., Nel JL, Ryan PG, Klages NT, Wilson RP, Robertson G (2000) Foraging ecology of grey-headed mollymawks at Marion Island, southern Indian Ocean, in relation to longline fishing activity. Biol Conserv 96:219-231.

Nel DC, Lutjeharms JRE, Pakhomov EA, Ansorge IJ, Ryan PG, Klages NTW (2001) Exploitation of mesoscale oceanographic features by grey-headed albatross *Thalassarche chrysostoma* in the southern Indian Ocean. Mar Ecol Prog Ser 217:15–26.

Pennycuick CJ (1982) The flight of petrels and albatrosses observed in South Georgia and its vicinity. Philos Trans R Soc B 300:75–106.

Perold V, Schoombie S, Ryan PG (2020) Decadal changes in plastic litter regurgitated by albatrosses and giant petrels at sub-Antarctic Marion Island. Mar Pollut Bull 159:111471.

Pinto JG, Fröhlich EL, Leckebusch GC, Ulbrich U (2007) Changing European storm loss potentials under modified climate conditions according to ensemble simulations of the ECHAM5/MPI-OM1 GCM. Nat Hazards Earth Syst Sci 7:165–175.

R Core Team (2021). R: A language and environment for statistical computing. R Foundation for Statistical Computing, Vienna, Austria. URL https://www.R-project.org/.

Richardson PL (2015) Upwind dynamic soaring of albatrosses and UAVs. Prog Oceanogr 130:146–156.

Richardson PL, Wakefield ED, Phillips RA (2018) Flight speed and performance of the wandering albatross with respect to wind. Mov Ecol 6:1–15.

Risi MM, Jones CW, Osborne AM, Steinfurth A, Oppel S (2021) Southern Giant Petrels *Macronectes giganteus* depredating breeding Atlantic Yellow-nosed Albatrosses *Thalassarche chlororhynchos* on Gough Island. Polar Biol 44:593–599.

Risi MM, Jones CW, Schoombie S, Ryan PG (2019) Plumage and bill abnormalities in albatross chicks on Marion Island. Polar Biol 42:1615–1620.

Robertson G, Moreno C, Arata JA, Candy SG, Lawton K, Valencia J, Wienecke B, Kirkwood R, Taylor P, Suazo CG (2014) Black-browed albatross numbers in Chile increase in response to reduced mortality in fisheries. Biol Conserv 169:319–333.

da Rocha N, Oppel S, Prince S, Matjila S, Shaanika TM, Naomab C, Yates O, Paterson JRB, Shimooshili K, Frans E, Kashava S, Crawford R (2021) Reduction in seabird mortality in Namibian fisheries following the introduction of bycatch regulation. Biol Conserv 253:108915.

Rodríguez A, Holmes ND, Ryan PG, Wilson K-J, Faulquier L, Murillo Y, Raine AF, Penniman JF, Neves V, Rodríguez B, Negro JJ, Chiaradia A, Dann P, Anderson T, Metzger B, Shirai M, Deppe L, Wheeler J, Hodum P, Gouveia C, Carmo V, Carreira GP, Delgado-Alburqueque L, Guerra-Correa C, Couzi F-X, Travers M, le Corre M (2017) Seabird mortality induced by land-based artificial lights. Conserv Biol 31:986–1001.

Ronconi RA, Allard KA, Taylor PD (2015) Bird interactions with offshore oil and gas platforms: Review of impacts and monitoring techniques. J Environ Manage 147:34–45.

le Roux PC (2008) Climate and climate change. In: *The Prince Edward Islands: Land-Sea Interactions in a Changing Ecosystem*. Chown SL, Froneman PW (eds) Stellenbosch University Press, Stellenbosch, pp 39–64.

Rudolph EM, Hedding DW, de Bruyn PJN, Nel W (2022) An open access geospatial database for the sub-Antarctic Prince Edward Islands. S Afr J Sci 118:77-84.

Ryan PG (1993) The ecological consequences of an exceptional rainfall event at Gough Island: news and views. S Afr J Sci 89:309–311.

Ryan PG, Bester MN (2008) Pelagic predators. In: *The Prince Edwards Islands: Land-sea Interactions in a Changing Climate*. Chown SL, Froneman PW (eds) Stellenbosch University Press, Stellenbosch, pp 121–164.

Ryan PG, Cooper J, Dyer BM, Underhill LG, Crawford RJM, Bester MN (2003) Counts of surface nesting seabirds breeding at Prince Edward Island, summer 2001/02. Afr J Mar Sci 20:441–451.

Ryan PG, Jones MGW, Dyer BM, Upfold L, Crawford RJM (2009) Recent population estimates and trends in numbers of albatrosses and giant petrels breeding at the sub-Antarctic Prince Edward Islands. Afr J Mar Sci 31:409–417.

Ryan PG, Phillips RA, Nel DC, Wood AG (2007) Breeding frequency in Grey-headed Albatrosses *Thalassarche chrysostoma*. Ibis 149:45–52.

Sachs G, Traugott J, Nesterova AP, Bonadonna F (2013) Experimental verification of dynamic soaring in albatrosses. 216:4222–4232.

Shepard E, Cole E, Neate A, Lempidakis E (2019) Wind prevents cliff-breeding birds from accessing nests through loss of flight control. eLife 8:e43842.

Shepard ELC, Ross AN, Portugal SJ (2016) Moving in a moving medium: new perspectives on flight. Philos Trans R Soc B 371:20150382.

Stahl JC, Sagar PM (2006). Behaviour and patterns of attendance of non-breeding birds at the breeding colony in a Buller's Albatross *Thalassarche bulleri* population at The Snares. Notornis 53:327–338.

Suryan RM, Anderson DJ, Shaffer SA, Roby DD, Tremblay Y, Costa DP, Sievert PR, Sato F, Ozaki K, Balogh GR, Nakamura N (2008) Wind, waves, and wing loading: Morphological specialization may limit range expansion of endangered albatrosses. PLoS One 3:e4016.

Tarroux A, Weimerskirch H, Wang S, Bromwich DH, Cherel Y, Kato A, Ropert-Coudert Y, Varpe Ø, Yoccoz NG (2016) Flexible flight response to challenging wind conditions in a commuting Antarctic seabird: do you catch the drift ? Anim Behav 113:99–112.

Taylor GK, Reynolds KV, Thomas ALR (2016) Soaring energetics and glide performance in a moving atmosphere. Philos Trans R Soc B 371:20150398.

Tickell WLN (1984). Behaviour of Black-browed and Grey-headed Albatrosses at Bird Island, South Georgia. Ostrich 55:64–85.

Tickell WLN (2000) Albatrosses. Pica Press, Sussex.

Tickell WLN, Pinder R (1975). Breeding biology of the Black-browed Albatross *Diomedea melanophris* and Grey-headed Albatross *D. chrysostoma* at Bird Island, South Georgia. Ibis 117:433–451.

US Department of Transportation FAA (2013) Glider Flying Handbook (FAA-H-8083-13). FAA Airman Testing Standards Branch, AFS-630, Oklahoma City.

Ventura F, Granadeiro JP, Padget O, Catry P (2020) Gadfly petrels use knowledge of the windscape, not memorized foraging patches, to optimize foraging trips on ocean-wide scales. Proc R Soc B 287:20191775.

Wand MP, Jones MC (1993) Comparison of Smoothing Parameterizations in Bivariate Kernel Density Estimation. J Am Stat Assoc 88:520–528.

Warham J (1977) Wing loadings, wing shapes, and flight capabilities of Procellariiformes. New Zeal J Zool 4:73–83.

Waugh SM, Weimerskirch H, Moore PJ, Sagar PM (1999) Population dynamics of Black-browed and Grey-headed Albatrosses *Diomedea melanophrys* and *D. chrysostoma* at Campbell Island, New Zealand, 1942-96. Ibis 141:216–225.

Weimerskirch H, Louzao M, de Grissac S, Delord K (2012) Changes in Wind Pattern Alter Albatross Distribution and Life-History Traits. Science 335:211–214.

Work TM, Duhr M, Flint B (2021) Pathology of house mouse (*Mus musculus*) predation on Laysan albatross (*Phoebastria immutabilis*) on Midway Atoll National Wildlife Refuge. J Wildl Dis 57:125–131.

Table 1: Numbers of grey-headed albatross carcasses found in Santa Rosa Valley in each of four breeding seasons in relation to adult and fledgling counts on Grey-headed Albatross Ridge. Also given are the number of new adult crash-landing mortalities and the estimated portion of the expected number of mortalities they represent.

Breeding season	Number of occupied nests	Number of chicks, pre-fledging	Number of fatal crash-landings[a]		Expected number of adult mortalities[b]	Crash estimated contribution to expected adult mortality	% of fledglings crash mortality
			Adults	Fledglings			
2017/18	4057	2052	64	28	398	16%	1%
2018/19	3993	1391	20	56	391	5%	4%
2019/20	3746	1808	43	44	367	12%	2%
2020/21	3643	1889	36	33	357	10%	2%
Mean	3860	1785	41	40	378	11%	2%
SD	171	244	16	11	17	4%	1%

[a] Only mortalities, no live grey-headed albatrosses included in these data

[b] Based on estimated adult survival rate of 95.1% for Marion Island (Converse et al. 2009)

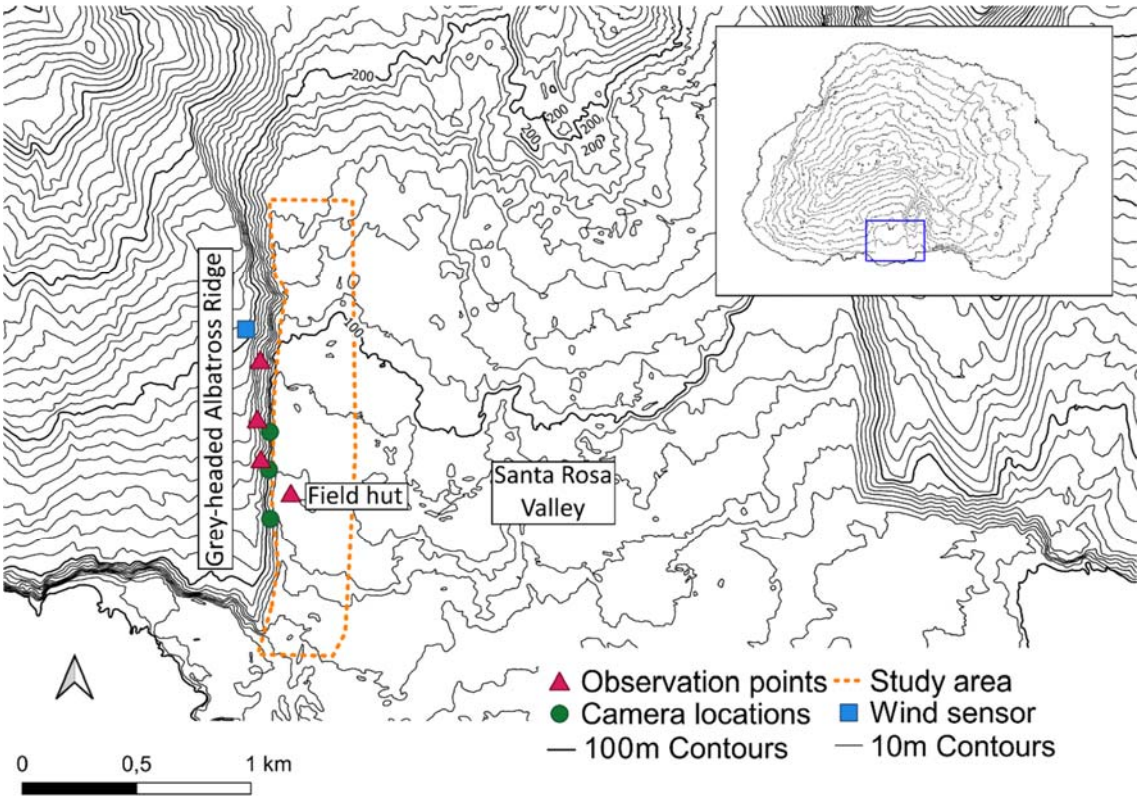

Fig. 1. Grey-headed Albatross Ridge and Santa Rosa Valley in 10 m contours (from Rudolph et al. 2022). The orange dashed block shows the carcass search area (i.e., the study area). The location of the wind sensor (blue square), observation points (pink triangles) and cameras (green circles) are shown on top of Grey-headed Albatross Ridge. Inset shows the location of the study area on Marion Island with 100 m contour lines.

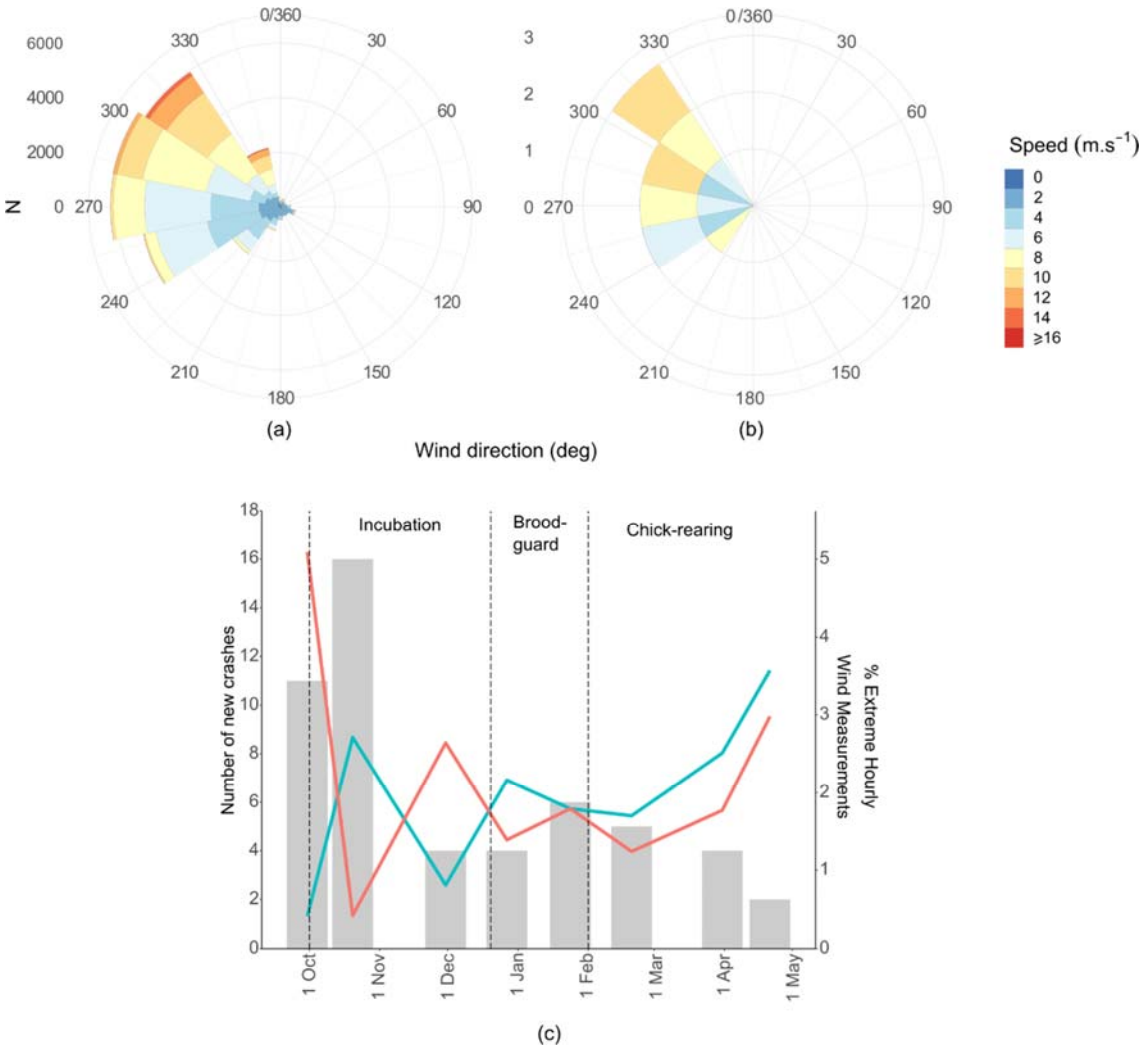

Fig. 2. Wind rose for the top of Grey-headed Albatross Ridge from August 2018 to April 2021 (a) and summary of mean wind speed and direction at the time of directly observed or recorded crash events (b). The number of new adult crashes for the 2019/20 breeding season (grey bar plots) given in relation to the number of extreme wind events (red lines) and calm conditions (blue lines) given as a percentage of all hourly measurements in the time between carcass surveys. Carcass survey data are reported as total values for each month, reported on the last day of the month on which any carcasses or live birds were recorded in the Valley for that month. Approximate periods for breeding phases are indicated with dashed black lines (c).

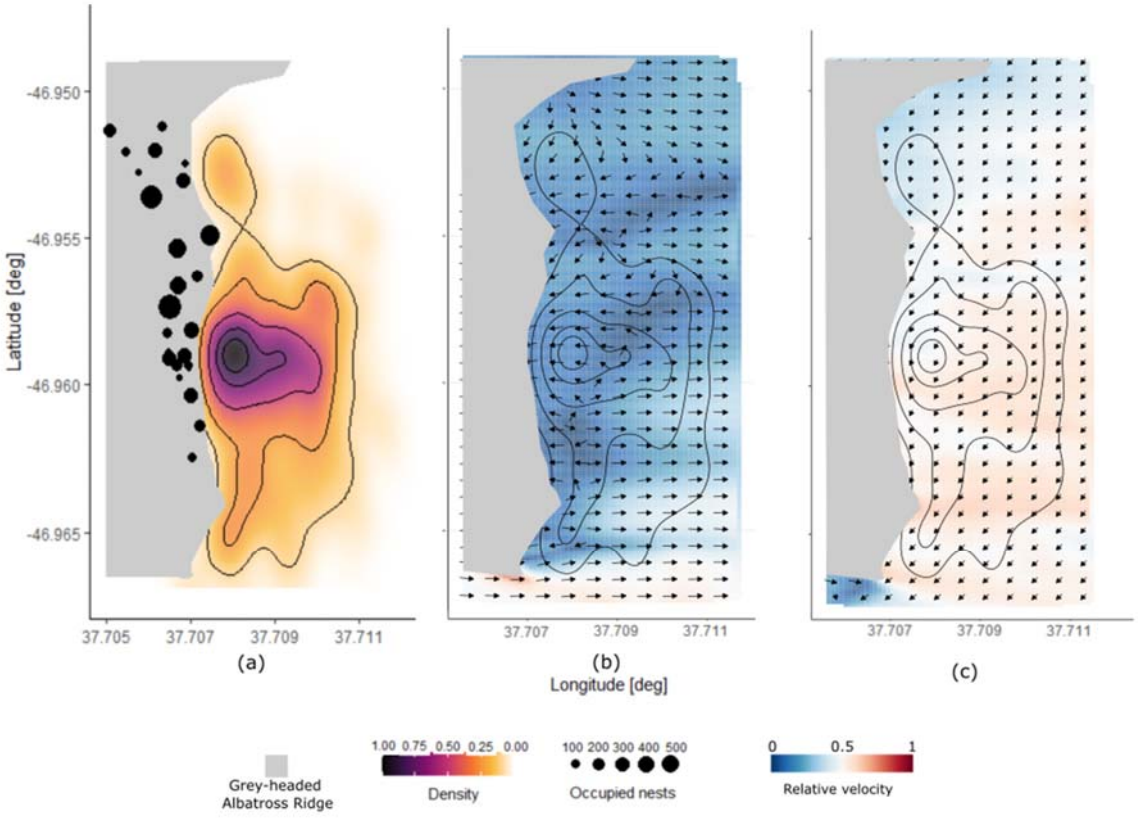

Fig. 3. Crash site density (contours 90th, 75th, 50th, 25th and 10th percentile) displayed relative to the outline of Grey-headed Albatross Ridge (grey area). The number of occupied nests at each colony, counted in late October 2019, is given in black dots, sized by the number of occupied nests (a). Two-dimensional wind fields (Goddard et al. 2022) at a constant height of 1 m.a.g.l. for the most and least prevalent wind directions, westerly (b) and north-easterly (c) respectively. Each grid point is denoted by an arrow indicating the wind direction (local wind direction) and background coloured by wind speed in the Long-Lat plane (referred to as the 2D-velocity). The velocity is given relative to a reference velocity (U_{ref} = 3 m.s^{-1}) as these simulation results can be scaled to represent changes in velocity and direction for a range of input velocity profiles.

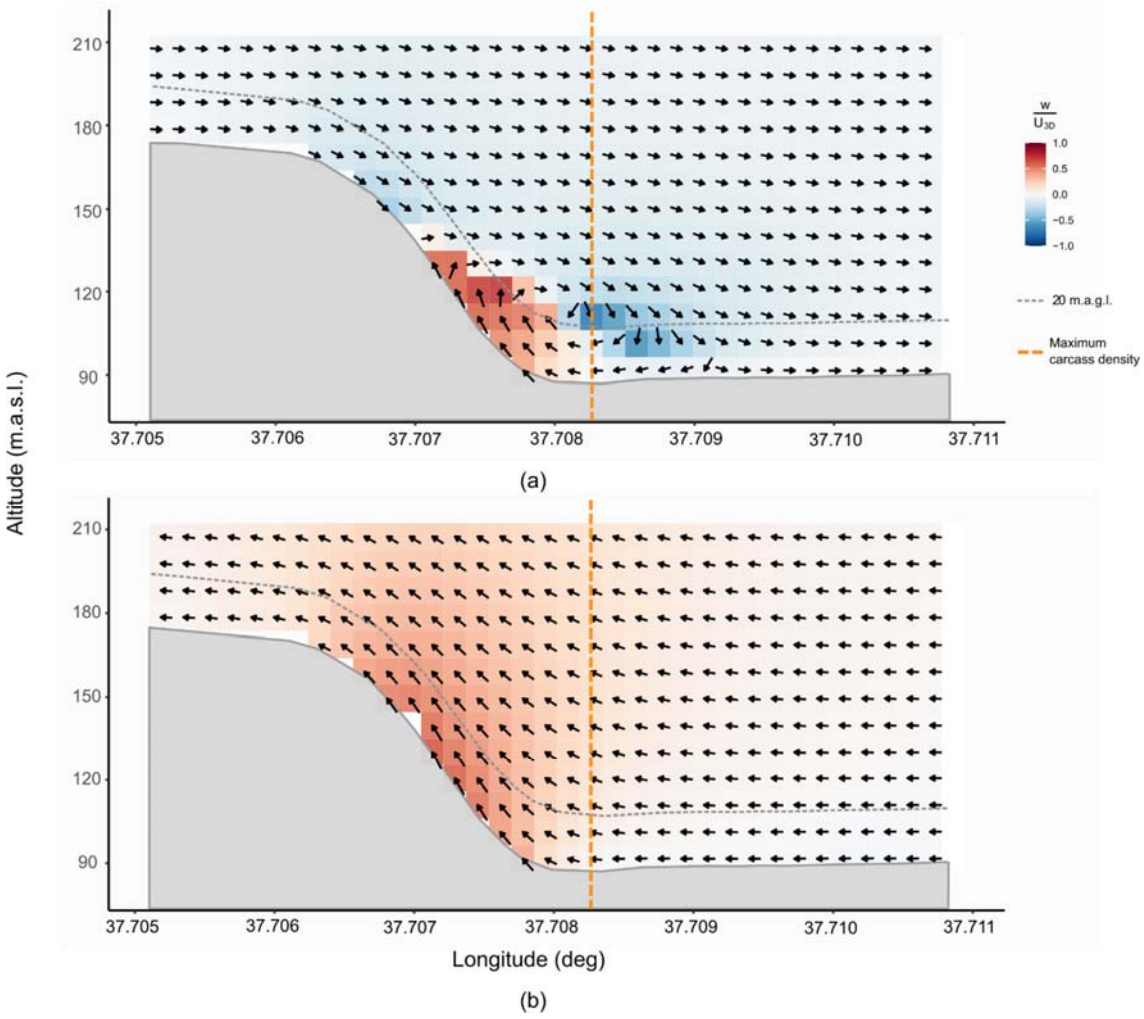

Fig. 4. Cross-section at a constant latitudinal line (-46.957°) corresponding to the maximum carcass density. Black arrows indicate two-dimensional vectors of the vertical and longitudinal velocity components, with the background tiles coloured by the vertical velocity component (w) as a proportion of the three-dimensional velocity magnitude (U_{3D}), for westerly (a) and easterly (b) winds. The grey area is an approximation of the Ridge slope at this latitude, the grey dashed line is a constant 20 m.a.g.l. line above the Valley and Ridge and the orange dashed line indicates the longitudinal line crossing the maximum carcass density.

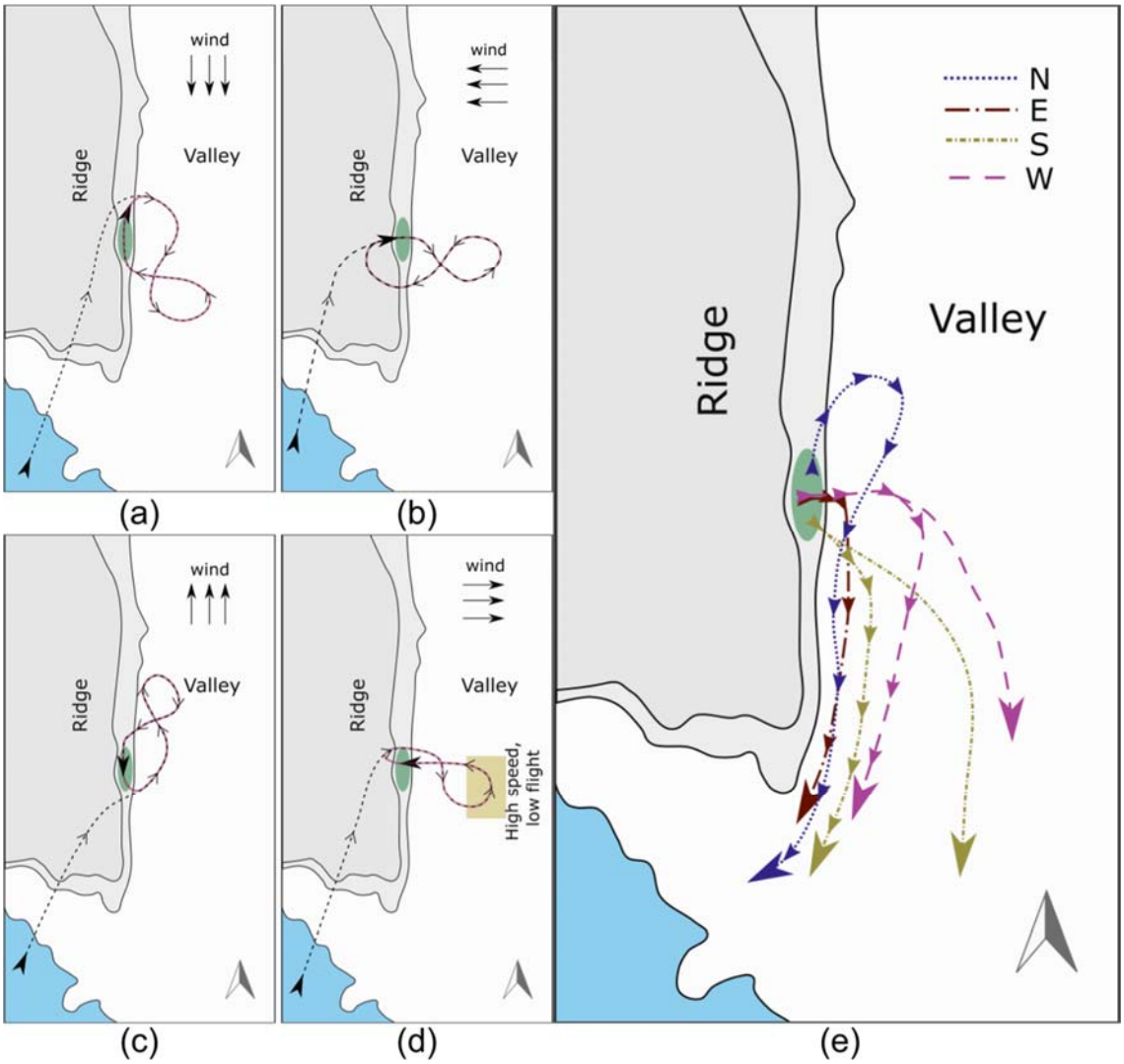

Fig. 5. Schematic flight paths of adult grey-headed albatrosses arriving at their breeding colony (green oval) on Grey-headed Albatross Ridge (Ridge) during moderate winds from the north (a), east (b), south (c), west (d) and departures from the Ridge, given for the four major wind sectors (e). Flight paths are approximate illustrations of birds arriving from/departing to the ocean (blue); looping paths (magenta) indicate the approximate flight path when multiple landing attempts are executed.